Clinical Article

Radiographic Features of Tumefactive Giant Cavernous Angiomas

Peter Kan, M.D.,[1] Marc Tubay, M.D.,[2] Anne Osborn, M.D.,[2] Susan Blaser, M.D.,[2] William T. Couldwell, M.D., Ph.D.[1]

[1]Department of Neurosurgery and [2]Department of Radiology, Division of Neuroradiology, University of Utah Health Sciences Center, Salt Lake City, Utah

Corresponding author: William T. Couldwell, M.D., Ph.D.

Department of Neurosurgery

University of Utah School of Medicine

175 N. Medical Drive East

Salt Lake City, UT 84132

Phone: 801-581-6908

Fax: 801-581-4138

Email: william.couldwell@hsc.utah.edu

Summary

Background. Giant cavernous angiomas (GCAs) are very rare, and imaging features of GCAs can be very different from those of typical cavernous angiomas (CAs), making them a diagnostic challenge. The purpose of the study was to evaluate the radiographic features of GCAs, with an emphasis on the differentiating features from neoplastic lesions.

Methods. The neuroradiological findings of 18 patients who harbored a histologically verified GCA (CA of 4 cm or larger) were reviewed retrospectively. The magnetic resonance imaging (MRI) appearance, enhancement pattern, presence of edema or mass effect, size, and location of each lesion was recorded. When available, pertinent clinical information, including age, sex, and mode of presentation, was obtained.

Findings. Seizures, neurologic deficits, hemorrhage, and hydrocephalus were the most common presenting symptoms. The lesions were hyperdense and nonenhancing on computed tomography with frequent calcifications. On MRI, the lesions most commonly had a multicystic appearance, representing blood of various ages, and multiple complete hemosiderin rings. GCAs can present in any location with associating edema and mass effect, giving them a tumefactive appearance. No developmental venous anomaly was observed with any lesion.

Conclusions. Most GCAs in our series presented as multicystic lesions with complete hemosiderin rings on MRI, giving a "bubbles of blood" appearance. Although this characteristic feature is helpful in the diagnosis of many cases of GCAs, the correct diagnosis in the remaining cases may not be apparent until histopathological evaluation of the specimen is made.

Key words: cavernous angiomas; cavernous malformations; giant; tumefactive

Running head: Radiographic features of tumefactive giant cavernous angiomas

Introduction

Cavernous angiomas (CAs) of the central nervous system (CNS) are angiographically occult vascular lesions. Their incidence is approximately 0.4% in modern magnetic resonance imaging (MRI) series (5), and they vary in size from a few millimeters to a few centimeters in diameter. Giant cavernous angiomas (GCAs) are very rare, with only 18 reported cases in the literature (1-4, 6-11). Patients with GCAs can present for medical treatment in infancy or adulthood, usually with symptoms of seizures, hemorrhage, mass effect, or neurologic deficits. Although these lesions may originate from smaller CAs as a result of successive intralesional hemorrhages, the exact pathophysiology of GCAs is unclear. Imaging features of GCAs can be very different from those of typical CAs, and these lesions can be mistaken as neoplasms, often making them a diagnostic challenge. The purpose of the study was to evaluate the radiographic features of GCAs, with an emphasis on the differentiating features from neoplastic lesions.

Clinical Material and Methods

With University of Utah Institutional Review Board approval, we reviewed the neuroradiology archive at the University of Utah to identify all patients with a histologically verified GCA. The archive represents a collection of cases (with clinical and radiographic information) submitted through various academic centers in North America. CGCA was defined as a CA that exceeded 4 cm in size on the preoperative MRI. All patients were treated between 1988 and 2006, and their records were reviewed retrospectively. The neuroradiological findings (including MRI and computed tomography [CT] when available) were reviewed through existing neuroradiological records at the University of Utah Medical Center. The MRI appearance, enhancement pattern, presence of edema or mass effect, size, and location of each lesion was recorded, and a concise

differential diagnosis of the lesion was offered. When available, pertinent clinical information, including age, sex, and mode of presentation (seizure, hemorrhage, or neurologic deficits), was obtained from the patients' medical records.

Results

The clinical presentation (available in 7 patients) and neuroradiological findings of the 18 patients in this series are summarized in Table 1. Of the 14 patients whose age and sex were available, 10 were male and 4 were female, and the mean age was 21.5 years. Of the 7 patients with information regarding clinical presentation, seizures (43%, 3/7), neurologic deficits (43%, 3/7), hemorrhage (71%, 5/7), and hydrocephalus (71% 5/7) were the most common presenting symptoms.

CT characteristics

Of the 11 patients who underwent a CT scan, a hyperdense lesion on the noncontrast study was identified in all cases. None of the lesions enhanced significantly, and calcification was found in 64% (7/11) of lesions (Fig. 1A,B).

MRI characteristics

The lesions appeared heterogeneous on all MRI sequences and none enhanced significantly after the administration of gadolinium. On T1-weighted images, the lesions most commonly exhibited predominant hyperintensity (56%, 10/18). On T2-weighted images, the lesions most commonly had a multicystic heterogeneous appearance (83%, 15/18), along with multiple complete hemosiderin rings (78%, 14/18) (Figs. 2A,B, 3A–C, 4A–C). In one case, the lesion had a "salt-

and-pepper" appearance on all sequences (Fig. 5A,B). No developmental venous anomaly was found on MRI imaging to be associated with any lesion.

Edema was present in 17% (3/18) of cases, and 56% (10/18) of lesions exerted mass effect on the surrounding brain or adjacent ventricular system. GCA can occur in any location (hemispheric, ventricular, thalamic, hypothalamic, cerebellar, and even extracranial), and their maximal diameter ranged from 4 to 11 cm.

In each case, the main radiographic differential diagnosis included an atypical vascular malformation and a hemorrhagic neoplasm.

Treatment

Of the 18 patients, 17 had undergone surgery with the goal of gross total resection if possible. Support was withdrawn on the remaining patient according to the family's wishes and autopsy confirmed the diagnosis of GCA.

Discussion

Giant cavernous angiomas are very rare. Including those described in our series, only 36 cases have been reported in the English-language literature (1-4, 6-11). Similar to those described in previously reported cases, the GCAs in our series occurred in all locations: hemispheric, ventricular, thalamic, hypothalamic, cerebellar, and even extracranial. All lesions were hyperdense to brain on noncontrast CT studies, and most had calcifications. Calcifications are

believed to be associated with hyalinization of sinusoidal walls of the CA. On MRI, most GCAs presented as nonenhancing multicystic lesions, representing blood of different ages, and had multiple complete hemosiderin rings, giving a characteristic "bubbles of blood" appearance. The lack of contrast enhancement may be due to the slow perfusion of CAs in general, and some authors advocate the use of high-dose, time-delayed contrast MRI studies (8). Other imaging patterns included a "salt-and-pepper" appearance in one patient. Edema or mass effect may also be present in patients harboring GCAs, mimicking neoplasms. Nevertheless, hyperdensity and calcification on CT and multicystic appearance with hemosiderin rings on MRI give clues to the correct diagnosis and differentiate GCAs from hemorrhagic neoplasms such as oligodendroglioma and metastasis.

Cavernous angiomas vary in size from a few millimeters to a few centimeters in diameter. Unlike giant aneurysms that are defined as having a diameter of 2.5 cm or more, GCA does not have a precise definition and those CAs at the large end of the spectrum are loosely referred to as "giant." In our study, we defined GCAs as lesions of 4 cm or more because, although arbitrary, we believe that this represents the threshold of the characteristic multicystic MRI appearance of GCAs. Moreover, a strict and uniform definition may also facilitate future reporting of these unusal lesions.

The exact etiology of GCAs and their mechanism of growth are unclear. We speculate that these lesions may develop from smaller CAs and grow via recurrent hemorrhages, followed by clot organization, pseudocapsule formation, and secondary expansion. The osmotic effect of the blood break-down products in the cyst is thought to be the mechanism behind such growth. The

result is the characteristic multicystic lesions with blood in different stages of degradation and the surrounding hemosiderin rings. Interestingly, developmental venous anomaly, which is often associated with CAs and is thought to play a role in their pathogenesis, was not observed with any of the GCAs in our series.

The clinical presentations of patients with GCAs and CAs are similar. Seizure, neurologic deficits, and hemorrhage are the most common presenting symptoms in both groups. The high incidence of hydrocephalus associated with GCAs is likely related to their size and proximity to the ventricles (44% of lesions in our series were either intra- or periventricular in location). The treatment of symptomatic GCAs is surgical, especially for lesions in noneloquent areas where gross total resection is possible.

Conclusions

Most GCAs in our series presented as multicystic lesions with complete hemosiderin rings on MRI, giving a "bubbles of blood" appearance. Although this characteristic feature is helpful in the diagnosis of many cases of GCAs, the correct diagnosis in the remaining cases may not be apparent until histopathological evaluation of the specimen is made.

References

1.   Anderson RC, Connolly ES, Jr., Ozduman K, Laurans MS, Gunel M, Khandji A, Faust PL, Sisti MB (2003) Clinicopathological review: giant intraventricular cavernous malformation. Neurosurgery 53:374-378; discussion 378-379

2.   Chicani CF, Miller NR, Tamargo RJ (2003) Giant cavernous malformation of the occipital lobe. J Neuroophthalmol 23:151-153

3.   Khosla VK, Banerjee AK, Mathuriya SN, Mehta S (1984) Giant cystic cavernoma in a child. Case report. J Neurosurg 60:1297-1299

4.   Lawton MT, Vates GE, Quinones-Hinojosa A, McDonald WC, Marchuk DA, Young WL (2004) Giant infiltrative cavernous malformation: clinical presentation, intervention, and genetic analysis: case report. Neurosurgery 55:979-980

5.   Porter RW, Detwiler PW, Spetzler RF, Lawton MT, Baskin JJ, Derksen PT, Zabramski JM (1999) Cavernous malformations of the brainstem: experience with 100 patients. J Neurosurg 90:50-58

6.   Sansone ME, Liwnicz BH, Mandybur TI (1980) Giant pituitary cavernous hemangioma: case report. J Neurosurg 53:124-126

7.   Siddiqui AA, Jooma R (2001) Neoplastic growth of cerebral cavernous malformation presenting with impending cerebral herniation: a case report and review of the literature on de novo growth of cavernomas. Surg Neurol 56:42-45

8.   Thiex R, Kruger R, Friese S, Gronewaller E, Kuker W (2003) Giant cavernoma of the brain stem: value of delayed MR imaging after contrast injection. Eur Radiol 13 Suppl 6:L219-225

9.   Thiex R, Kruger R, Friese S, Gronewaller E, Kuker W (2003) Giant cavernoma of the brain stem: value of delayed MR imaging after contrast injection. Eur Radiol 13 Suppl 4:L219-225

10.   van Lindert EJ, Tan TC, Grotenhuis JA, Wesseling P (2007) Giant cavernous hemangiomas: report of three cases. Neurosurg Rev 30:83-92; discussion 92

11.   Voelker JL, Stewart DH, Schochet SS, Jr. (1998) Giant intracranial and extracranial cavernous malformation. Case report. J Neurosurg 89:465-469
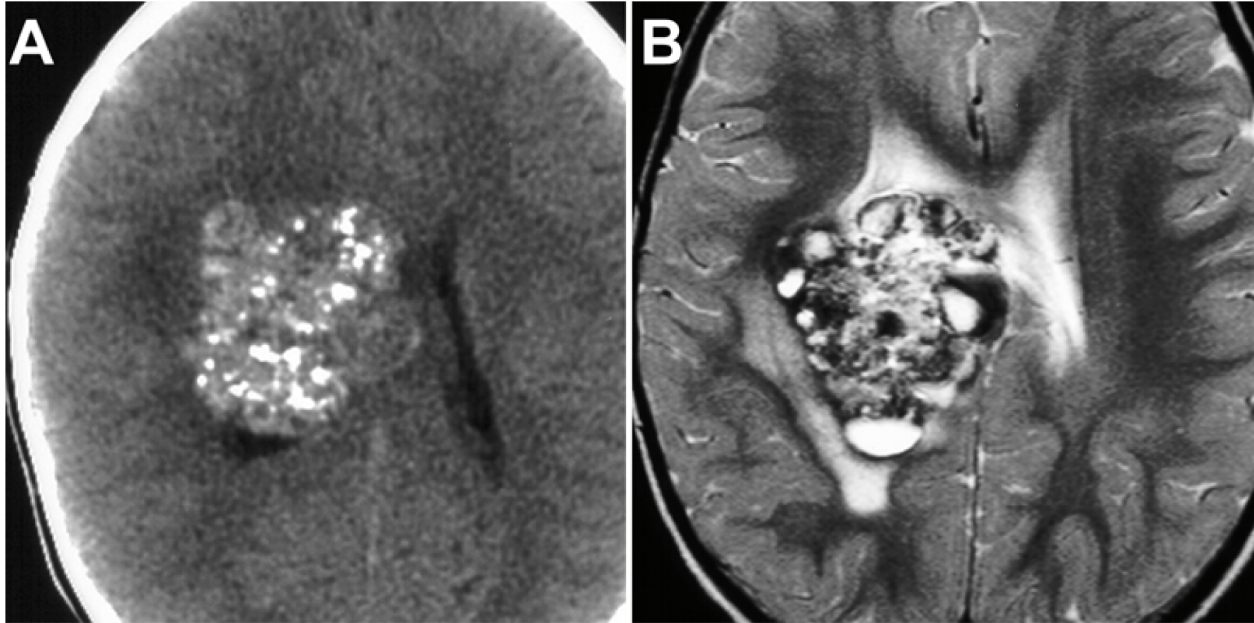
Fig. 1. Axial non-contrast CT scan (A) of case 18 revealed a deep, hyperdense right mesial frontal lesion with punctate calcification. Initial diagnosis was oligodendroglioma. After the visualization of the lesion on axial T2 imaging (B), the diagnosis was changed to GCA.
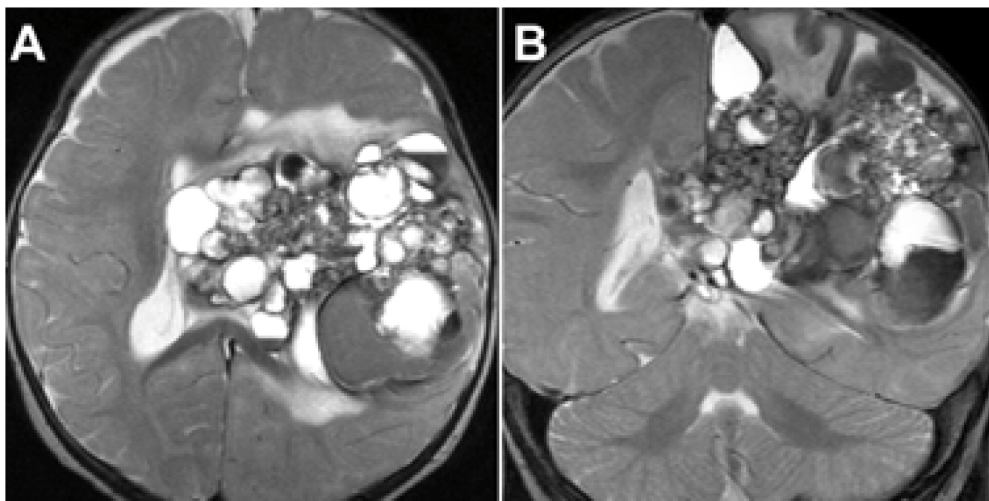

Fig. 2. Axial (A) and coronal (B) T2-weighted images of the patient presented in case 1 showing a large left frontoparietal GCA with its characteristic multicystic appearance. Note fluid–fluid levels caused by layering of chronic blood products within the cysts. The cysts are surrounded by complete rims of hemosiderin.

Fig. 3. Axial (A), sagittal (B), and coronal (C) T2-weighted images of the patient in case 6 demonstrating an enormous bifrontotemporal GCA with its characteristic multicystic appearance and complete hemosiderin rims.
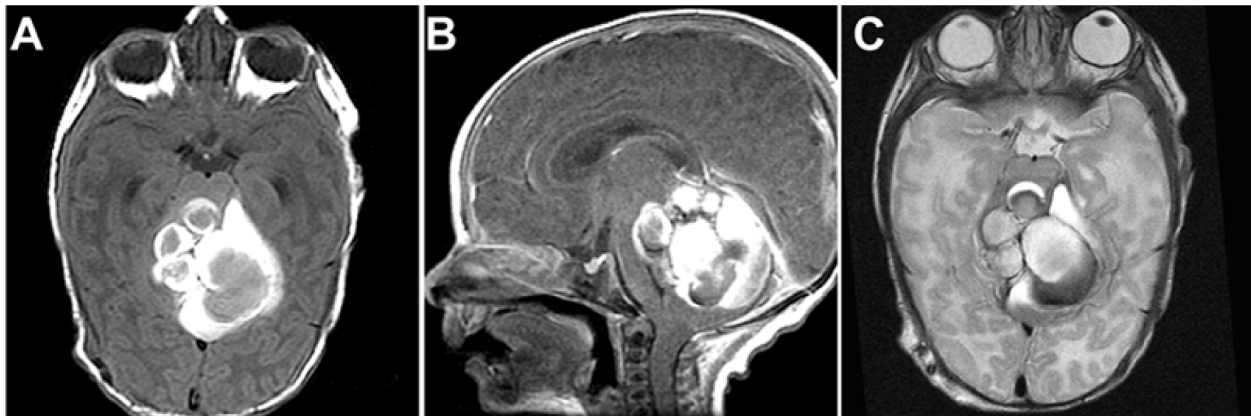

Fig. 4. Axial T1-weighted noncontrast (A), sagittal T1-weighted contrast-enhanced (B), and axial T2-weighted (C) images of the patient in case 12 revealed a large nonenhancing cerebellar GCA with its characteristic multicystic appearance.
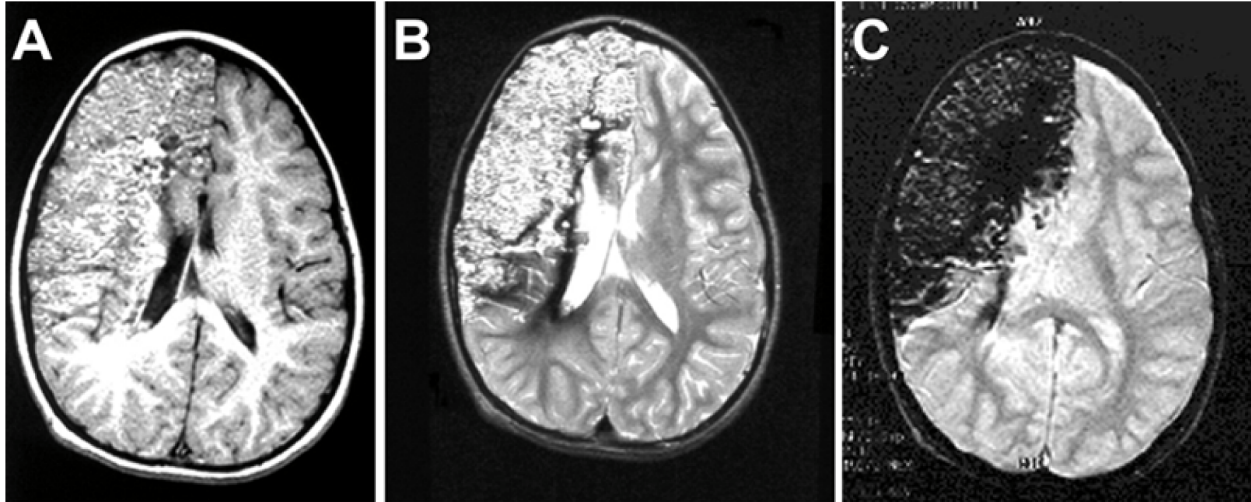
Fig. 5. Axial T1-weighted (A) and axial T2-weighted (B) images of the patient described in case 3 illustrating a GCA that occupies most of the right cerebral hemisphere with a salt-and-pepper appearance. The T2-weighted (B) and GRE (C) images showed profound hypointensity caused by extensive hemosiderin deposition.

Table 1. Clinical presentation and radiological findings of 18 patients with histologically verified GCA

Case no.: age (years)/sex	MRI appearance	CT appearance	Enhancement pattern	Presence of edema	Size (cm)	Location	Mass effect	Hemorrhage	Diagnosis	Clinical history	Treatment
1: 0.9/M	Hyperintense on T1, multicystic with multiple hemosiderin rings on T2, hyperintense on FLAIR, hypointense on GRE	Hyperdense, heterogeneous, calcification	N/A	Y	9X6	Left frontoparietal, intraventricular, crosses midline	Y	Y	Vascular malformation vs. neoplasm	Macrocrania (>98%), 3 week history of change in vision and mental status, seizure, and hemiparesis	Surgery
2: 23/M	Hyperintense on T1, multicystic with multiple hemosiderin rings on T2, hyperintense on FLAIR, hypointense on GRE	Hyperdense, heterogeneous	None/ minimal	N	4X3	Left frontal	N	N	Vascular malformation vs. neoplasm	N/A	Surgery
3: 9/M	Isointense, salt-and-pepper appearance on T1, hyperintense, salt-and-pepper appearance with flow voids on T2 + a dark rim of hemosiderin	Hyperdense, heterogeneous, calcification	None/ minimal	N	11X5	Right frontotemporoparietal	N	N	Vascular malformation vs. neoplasm	Progressive left hemiparesis, seizures, failure-to-thrive	Surgery
4 43/M	Isointense on T1, multicystic with multiple hemosiderin rings on T2, hyperintense on FLAIR, hypointense on GRE	Hyperdense, heterogeneous, punctate calcification	None/ minimal	N	4X3	Right parietal	N	N	Vascular malformation vs. neoplasm	N/A	Surgery
5: 30/M	Heterogeneous, hyperintense on T1, multicystic with multiple hemosiderin rings on T2, hypointense on GRE	N/A	None/ minimal	Y	3X3 to 6X5.5 in 41 days	Left deep parietal, extending down to the left thalamus	Y	Y	Vascular malformation vs. hemorrhagic neoplasm	Seizure, right sided weakness	Surgery
6: 1 day/M	Heterogeneous, hyperintense on T1, multicystic with multiple hemosiderin rings on T2	Hyperdense, heterogeneous	None/ minimal	N	11X9	Bifrontotemporoparietal	Y	N	Vascular malformation vs. neoplasm	Macrocephalic, tense fontanelle, flaccid X 4, and intubated for apneic episodes; care withdrawn (autopsy proven CA)	No treatment, support withdrawn
7: 25/F	Heterogeneous, hyperintense on T1, multicystic on T2, hypointense on GRE	N/A	None/ minimal	N	4X3X3	Left cerebellum, paramedian	Y	Y	Vascular malformation vs. hemorrhagic neoplasm	Headache, nausea/vomiting, hydrocephalus	Surgery
8: 44/F	Heterogeneous, hyperintense on T1, multicystic on T2, hypointense on GRE	Hyperdense, heterogeneous	None/ minimal	N	4X3	Hypothalamic/third ventricular	N	Y	Vascular malformation vs. hemorrhagic neoplasm	Sudden onset of headache, then obtunded, hydrocephalus	Surgery
9:	Heterogeneous,	N/A	None/	N	4X3	Cerebellum,	Y	N	Vascular	N/A	Surgery

Age/Sex	MRI	CT	Enhancement		Size	Location			Diagnosis	Symptoms	Treatment
0.2/M	hyperintense on T1, multicystic with multiple hemosiderin rings on T2		minimal			paramedian			malformation vs. neoplasm		
10: 66/M	Heterogeneous, isointense on T1, multicystic with multiple hemosiderin rings on T2, heterogeneous hyperintense on FLAIR, hypointense on GRE	N/A	None/minimal	N	4X3	Right lateral ventricle	Y	Y	Vascular malformation vs. neoplasm	N/A	Surgery
11: 25/F	Hypointense on T1/T2	N/A	None/minimal	N	5X4	Right frontal extra/intracranial	N	N	Vascular malformation vs. neoplasm	N/A	Surgery
12: 0.1/M	Hyperintense on T1, multicystic with multiple hemosiderin rings on T2, hyperintense on FLAIR.	Hyperdense, heterogeneous, calcification	None/minimal	N	6X6	Cerebellum	Y	N	Vascular malformation vs. neoplasm	Irritability, bulging fontanelle (hydrocephalus)	Surgery
13: 16/F	Hyperintense on T1, multicystic with multiple hemosiderin rings on T2	N/A	None/minimal	N	4X4	Left thalamic, extending down to the left midbrain	Y	N	Vascular malformation vs. neoplasm	N/A	Surgery
14: 19/M	Hyperintense on T1, hetereogeneous on T2	Hyperdense, consistent with hemorrhage	None/minimal	Y	4X4	Left frontal	Y	Y	Hemorrhagic neoplasm	N/A	Surgery
15: N/A	Heterogeneous on T1, multicystic with multiple hemosiderin rings on T2	N/A	None/minimal	N	5X4	Left cerebellar, extending into the left pons	N	N	Vascular malformation vs. neoplasm	N/A	Surgery
16: N/A	Heterogeneous on T1, multicystic with multiple hemosiderin rings on T2	Hyperdense with punctate calcification	None/minimal	N	4X4	Right atrium	N	N	Vascular malformation vs. neoplasm	N/A	Surgery
17: N/A	Heterogeneous on T1, multicystic with multiple hemosiderin rings on T2	Hyperdense with punctate calcification	None/minimal	N	4X4	Right caudate, thalamic, bilateral lateral ventricles	N	N	Vascular malformation vs. neoplasm	N/A	Surgery
18: N/A	Heterogeneous on T1, multicystic with multiple hemosiderin rings on T2	Hyperdense with punctate calcification	None/minimal	N	4X4	Right-sided, deep mesial frontal	Y	N	Vascular malformation vs. neoplasm	N/A	Surgery

N/A: Not available; FLAIR: fluid-attenuated inversion recovery; GRE: gradient echo imaging; GCA: giant cavernous angioma